4/18/2023

Report on the Potential Impact of Partial Development of Fanling Golf Course Site on Groundwater Flow System

Professor Jiu Jimmy Jiao
THE DEPARTMENT OF EARTH SCIECNES, THE UNIVERSITY OF HONG KONG

Table of Contents

1 INTRODUCTION

1.1 Background of this project

The potential development area for public housing and supporting infrastructure is situated within the Fanling Golf Course (FGC), covering 32 hectares (0.32 km2), specifically east of Fan Kam Road, and referred to as East FGC. The area is divided into four sub-areas, as shown in Figure 1, based on the 2019 Environmental Impact Assessment (EIA) [*Civil Engineering and Development Department (CEDD)*, 2019]. According to the EIA, sub-area 1 has low-to-moderate ecological value, making it suitable for housing development. On the other hand, sub-area 4 has an overall ecological value assessed as moderate to high, mainly due to a swampy woodland of about 1.4 hectares along the fairways and the presence of 38 Chinese swamp cypresses. These cypresses are classified as Class I protected species in China and are globally critically endangered, requiring a specialized habitat and are sensitive to changes in the water table.

The housing foundation typically reaches into bedrock and utilizes construction materials which are almost impermeable. Previous studies have shown that using deep foundations, which replace the shallow soil above bedrock with construction materials, can obstruct groundwater flow and possibly increase water levels at the upstream of the foundation [*Ding et al.*, 2008; *Jiao et al.*, 2006]. Therefore, it is necessary to investigate how the building foundation impacts the groundwater flow system as part of assessing the ecological impact of housing development in sub-area 1. Additionally, to compensate for the loss of trees in sub-area 1, planting trees in sub-areas 2 and 3 has been proposed. The potential impact of this compensatory tree planting on the groundwater flow system will also be evaluated.

This project aims to develop a three-dimensional (3D) regional groundwater flow model that centers on the potential development area for public housing and supporting infrastructure in sub-area 1. The 3D groundwater flow model will be used to assess the hydrological impact of housing development in sub-area 1 and the potential compensatory tree planting in sub-areas 2 and 3.

1.2 Objectives of this project

This project covers the following works:

1) Collect geological borehole logging data from CEDD library.

2) Collect hydraulic conductivity and water level data from the CEDD library.

3) Conduct K-sat experiments at 12 golf course sites to measure the hydraulic conductivity of the unsaturated shallow soil.

4) Conduct falling-head tests at the newly drilled boreholes at the golf course site to measure the hydraulic conductivity.

5) Build a 3D hydrogeological model to simulate the groundwater flow before the housing development in sub-area 1 and calibrate the model by the collected water level data.

6) Predict the water level change in East FGC after the construction of buildings in sub-area 1

7) Predict the future water level change in East FGC after the construction of buildings in sub-area 1 and the compensatory tree planting in East FGC.

The project also examined the impact of the development on Long Valley Nature Reserve at the north of the golf site. Overall, the project provides a comprehensive understanding of the hydrological impact of housing development on the water level in the swampy woodland and Long Valley Nature Reserve.

2 DATA COLLECTION

2.1 Summary of data collection

The data collected for the project include three types: borehole logging data, water level data, and hydraulic conductivity data.

As shown in Figure 1, 101 borehole logging data were collected from the CEDD library, and 6 extra borehole logging data were collected from the boreholes which were drilled by CEDD recently in sub-areas 1-4 for their detailed analysis of the hydrological impact.

For water level data, 24 were taken from the CEDD library, and 6 were obtained at the newly drilled boreholes in sub-areas 1-4 (Figure 2).

Hydraulic conductivity data were collected from three sources: 12 from K-sat experiments we carried out at the golf courses, 25 falling-head test data from the CEDD library, and 3 falling-head test data measured by us at the newly drilled boreholes (Figures 3 and 4). Furthermore, the hydraulic conductivity data can be classified into two categories: hydraulic conductivity data at the shallow unsaturated soil layer (12 K-sat data and 5 from CEDD library), and the hydraulic conductivity data at the weathered bedrock layer (20 from CEDD library and 3 from newly drilled borehole in sub-areas 1-4).

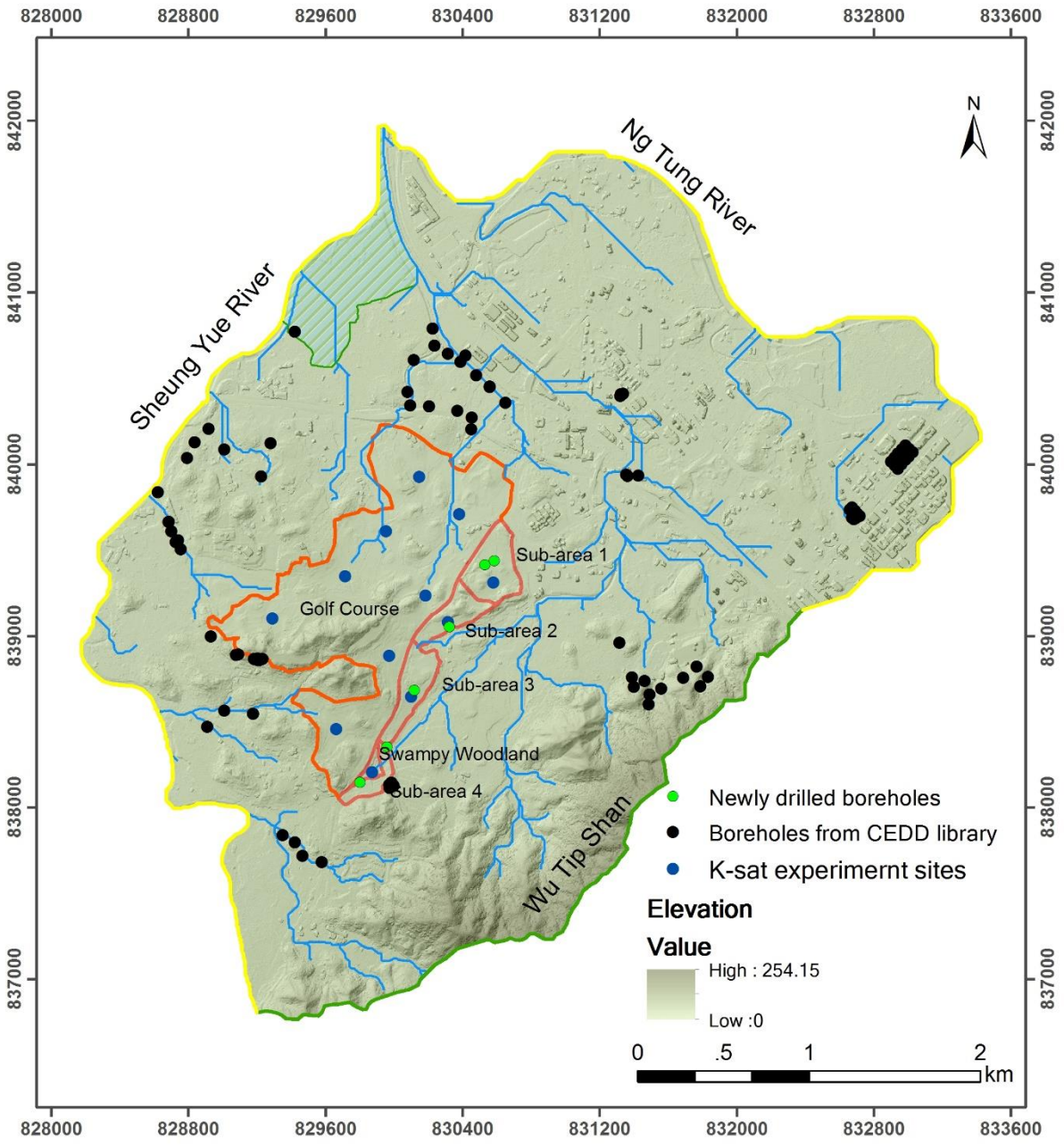

Figure 1. Locations of boreholes with data collected from CEDD library, Ksat test sites, and 6 newly drilled boreholes at sub-areas 1-4

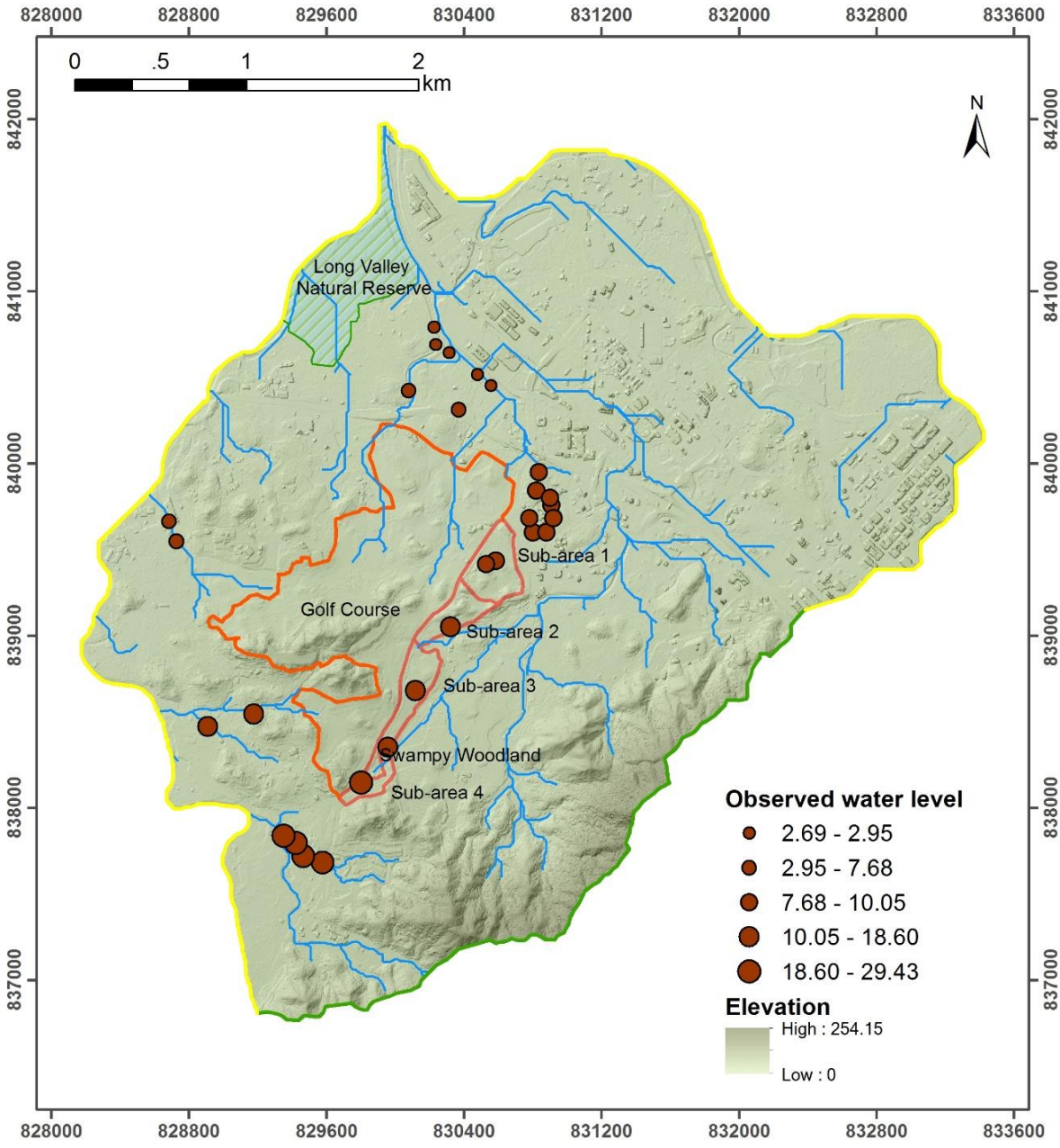

Figure 2. Spatial distribution of boreholes with water level data.

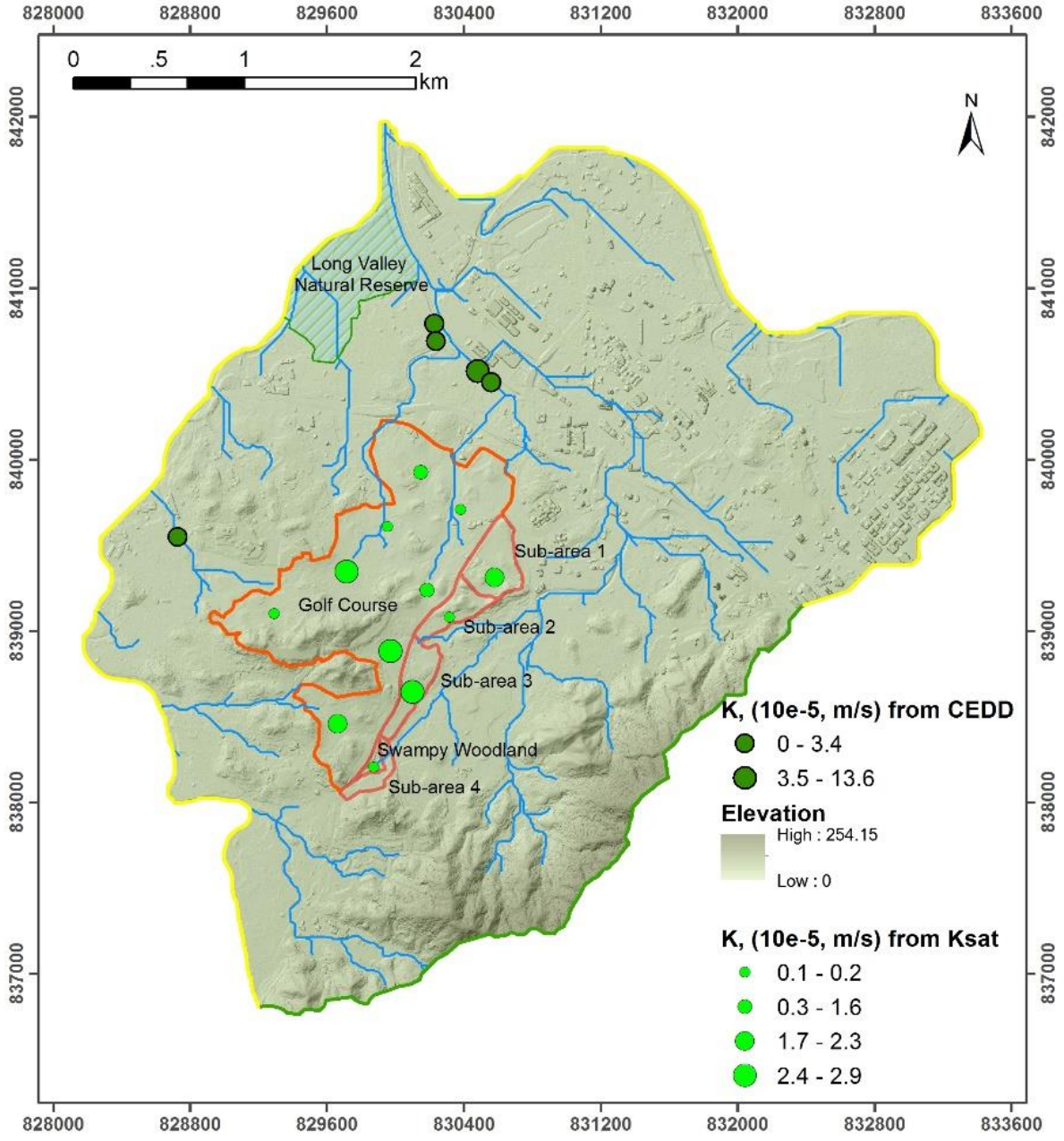

Figure 3. Locations of the sites with hydraulic conductivity data in the shallow soil layer

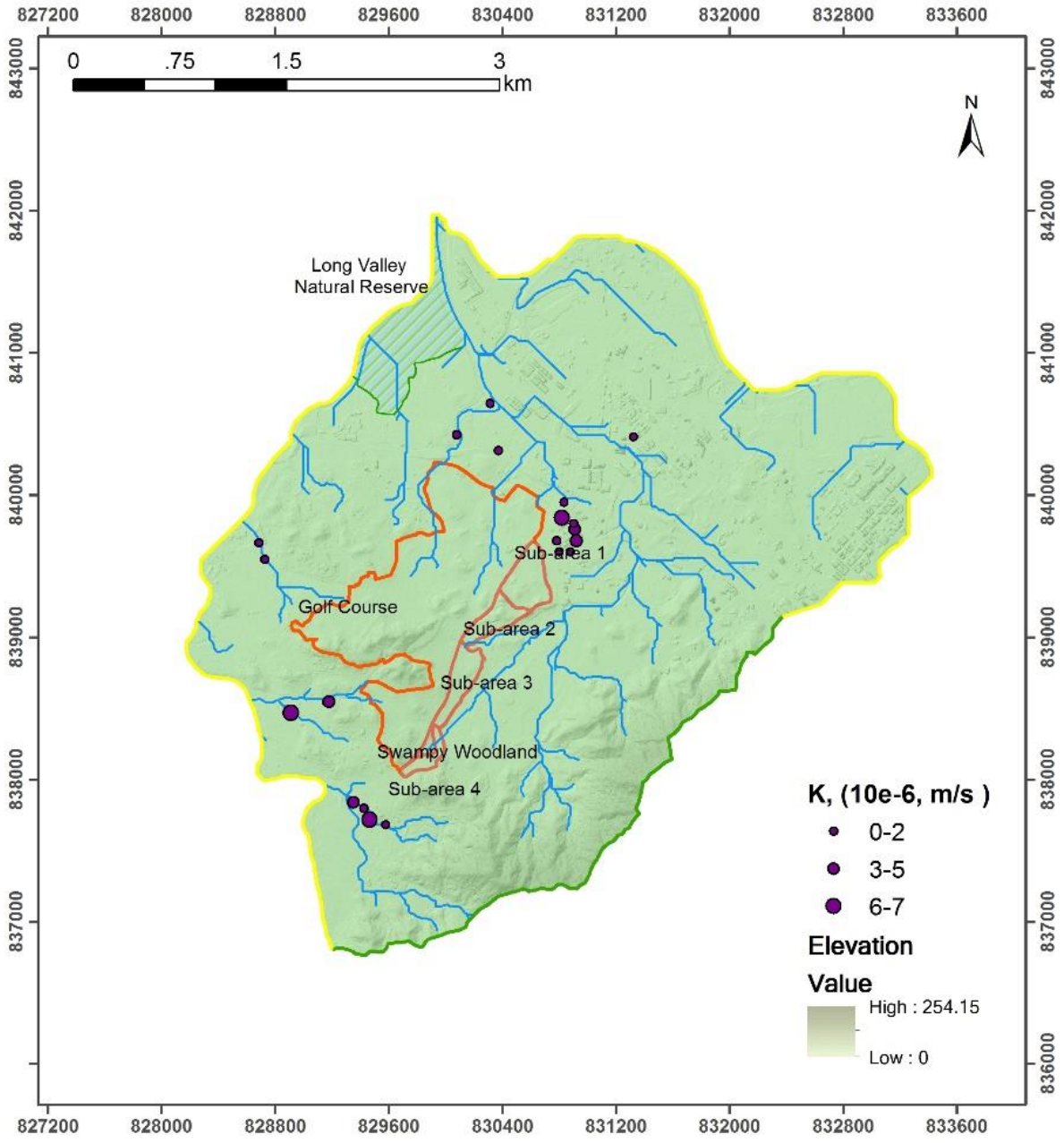

Figure 4. Locations of the sites with hydraulic conductivity data in the weathered bedrock.

2.2 K-sat experiments at the golf course

The K-sat experiment is a method for determining the saturated hydraulic conductivity (Ksat) of the unsaturated zone in soil. It is conducted using a Compact Constant Head Permeameter (CCHP),

also known as the Amoozemeter (Figures 5 and 6) [*Equipment*, 2004]. This field instrument is capable of measuring Ksat from the soil surface to a depth of 2 m. The Glover solution is used to calculate Ksat. The Glover solution is evaluated using the depth of water in the hole (H), the radius of the hole (r), and one measurement of the steady-state flow rate (Q). Specifically, the Glover solution is given by:

$$K_{sat} = AQ$$

where

$$A = \left\{ \sinh^{-1}\left(\frac{H}{r}\right) - \left[\left(\frac{r}{H}\right)^2 + 1\right]^{1/2} + \frac{r}{H} \right\} / (2\pi H^2)$$

To conduct the K-sat experiment, a hole is made using a hand auger, and a constant-head tube is filled with water. The desired depth of water in the hole is controlled by the adjustable bubble tube. The water dissipating unit is then lowered to the bottom of the hole, and the three-way valve is opened to allow water to flow into the auger hole. When a constant head of water is established in the hole, the depth of water in the hole is determined, and the change in water level in the flow measuring reservoir with time is recorded. After three consecutive steady-state flow rates are measured, the depth of water in the hole is measured again, and the Ksat value is calculated using the Glover solution.

The saturated hydraulic conductivities in soil measured at Fanling golf course sites are listed in Table 1 and shown in Figure 3.

Table 1. Saturated hydraulic conductivities (m/s) of shallow soil measured at Fanling golf course site

E18	E17	E10	E15	N14	O17
6.8×10^{-7}	2.1×10^{-6}	2.6×10^{-5}	2.0×10^{-6}	1.6×10^{-5}	1.5×10^{-5}
O15	**O12**	**O2**	**O4**	**O6**	**O7**
2.6×10^{-5}	2.0×10^{-5}	2.3×10^{-5}	1.2×10^{-6}	2.8×10^{-5}	9.1×10^{-7}

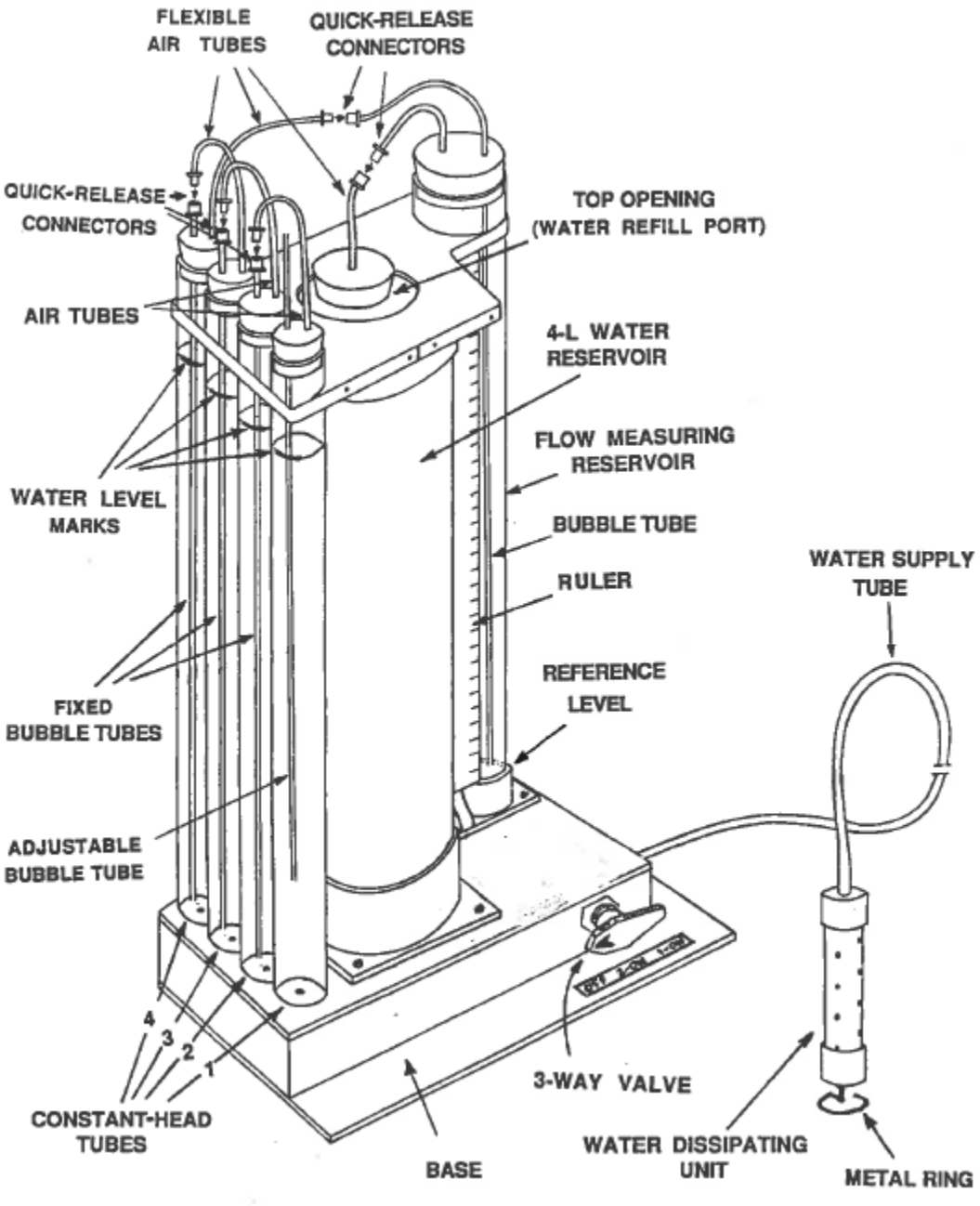

Figure 5. Various components of CCHP

Figure 6. HKU team conducting K-sat experiment at Fanling golf course site.

2.3 Falling-head test at the newly drilled borehole in sub-areas 1-4

After the boreholes drilled at sub-areas 1-4 by CEDD, falling-head tests were conducted in these holes to estimate the hydraulic conductivity., The test involved an instantaneous change in water level in the boreholes, followed by measurement of the rate at which the water level returns to its initial level (Figure 7).. The faster the return to initial head, the higher the hydraulic conductivity.

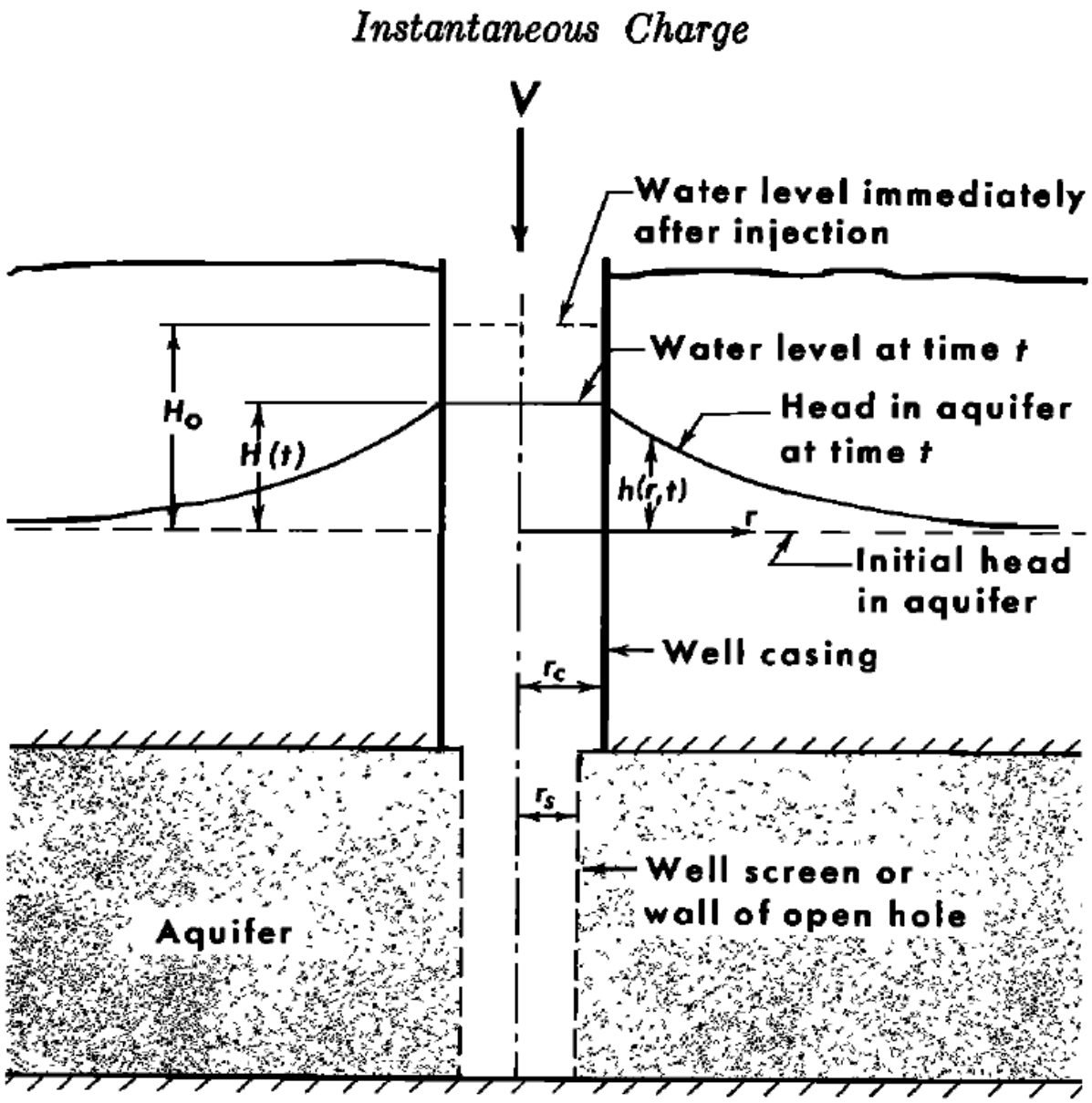

Figure 7. Water level change during a falling-head test

Figure 8. HKU team conducting Falling-head test at the Fanling golf course sites

To conduct the test, various apparatuses are required, including the facilities to add water, water table indicator (dip meter), and pressure transducer. Field procedures for conducting the test involve measuring the initial water level (H_0) in the well, lowering the transducer to an appropriate depth, introducing the slug, and measuring the water level recovery curve.

Data processing is based on the obtained water level recovery curve. The Hvorslev method is applied to calculate the hydraulic conductivity in this study, which includes reading the value of T_0, the basic time lag, from the water level recovery curve. T_0 is the time at which the head ratio (H/H_0) equal to 0.37. The value of K, which represents the hydraulic conductivity of the formation, can then be calculated using a formula below:

$$K = \frac{r^2 \ln(L/R)}{2LT_0}$$

Where r is the radius of the well or piezometer casing, L is the length of the saturated portion of the screen or filter pack, R is the radius of the screen or screen plus filter pack.

The calculated hydraulic conductivities at the newly drilled boreholes are 4.61×10^{-6} m/s at GBH1, 1.60×10^{-6} $/s$ at GBH2, and 7.57×10^{-7} m/s at GBH6.

3 GROUNDWATER FLOW SIMULATION

3.1 Construction of 3D hydrogeological model

3.1.1 Model area

The main concerned area in this study is elongated portion of the Fanling Golf Course, or aub-areas 1-4 shown in Figure 1. This concerned area spans over 0.32 km^2, with a length of 1.9 km and a width of up to 300 m. Since groundwater flow in this area is part of a larger regional system, the model area must cover a broader region.

To determine the model area for the simulation of groundwater flow, high-resolution DEM data was used to identify watersheds around the Fanling Golf Course site. The Wu Tip Shan mountain ridge, serving as a water divide for surface runoff, was selected as the southeast boundary of the model, as depicted in Figure 1. The Shueng Yue River was chosen as the west boundary, while the Ng Tung River was selected as the northeast boundary. These are all natural boundaries, allowing for straightforward determination of boundary conditions for groundwater flow. Additionally, these boundaries are located at a reasonable distance from the golf course, resulting in minimal uncertainty impacts. Ultimately, the total model area comprises 15.43 km^2. Further elaboration of the boundary conditions will be provided in the boundary condition section.

3.1.2 Model stratification

The hydrogeological model is constructed using the borehole logging data from CEDD library shown in Figure 1, based on which the stratigraphy in the study area can be approximated by a three-layer structure. Layer 1 consists of fill material, colluvium, and alluvium. Layer 2 is composed of completely and highly decomposed tuff with Grade IV-VI. Layer 3 consists of moderately to fresh bedrock with Grade I-III. To establish a 3D hydrogeological model, the thicknesses of layers 1 and 2 are determined based on the borehole data.

The relationship between the thickness of the first layer and the ground elevation has been analyzed and presented in Figure 9. It was observed that the thickness of the first layer is relatively uniform

when the ground elevation is higher than 30 mPD. However, it shows a significant spatial variation when the ground elevation is lower than 30 mPD. Based on this analysis, the 3D hydrogeological model of the first layer has been determined, and the mean thickness of the first layer above 30 mPD is estimated to be 1.09 m based on the logging data from the boreholes located above 30 mPD. On the other hand, the mean thickness of the first layer below 30 mPD is estimated to be 7.20 m based on the logging data from the borehole below 30 mPD, which indicates that there is a significant increase in the thickness of the first layer as the elevation decreases. Figure 11 shows the bottom elevation of the first layer in the 3D hydrogeological model.

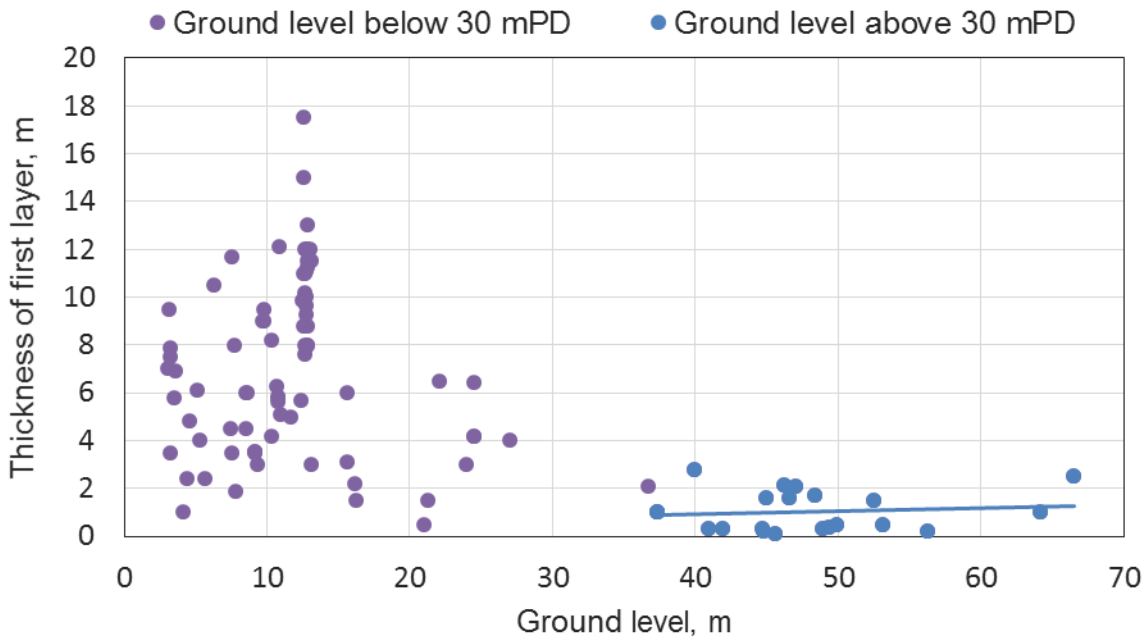

Figure 9. Relation between the thickness of the first layer and ground elevation based on the borehole logging data

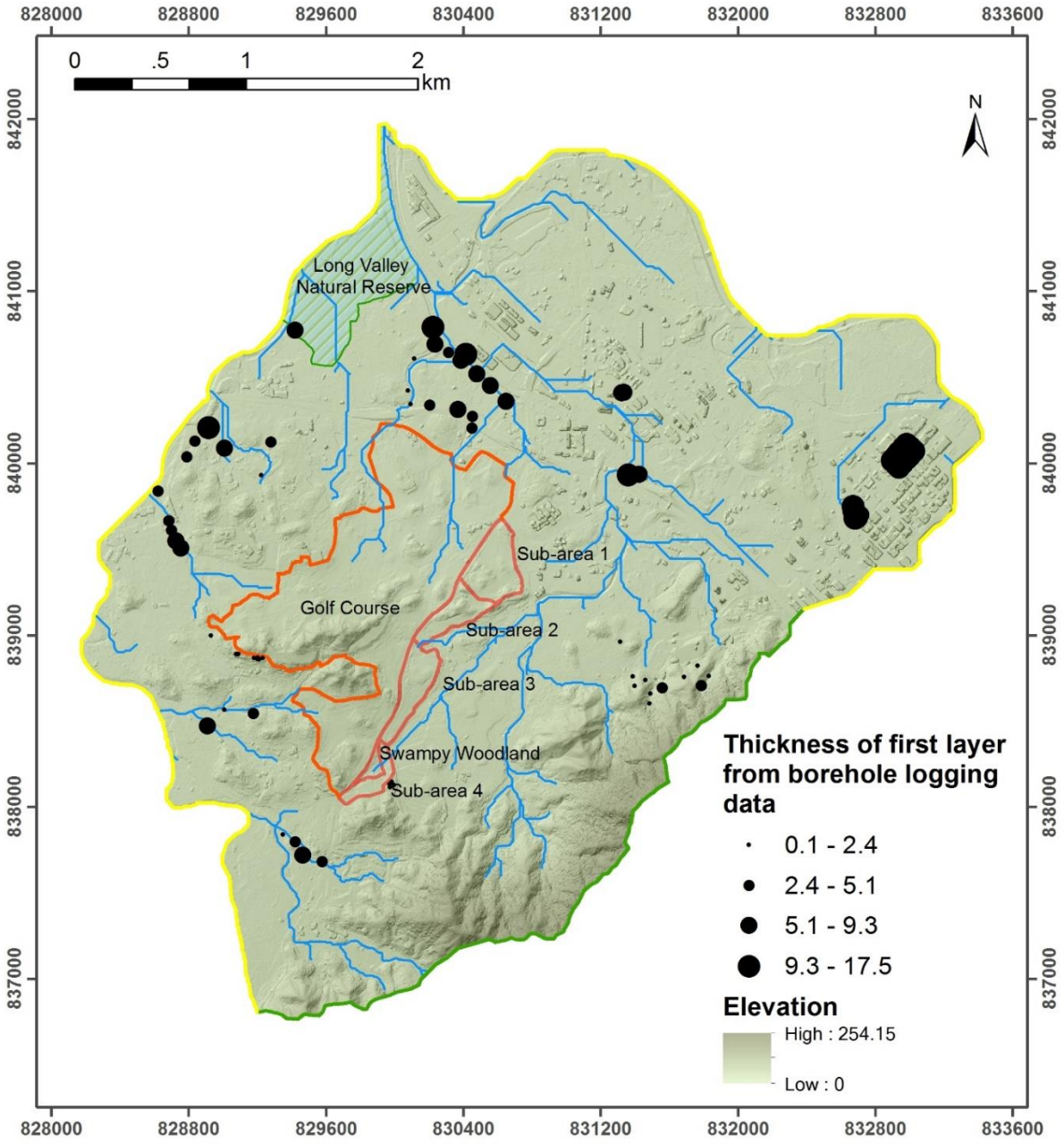

Figure 10. Spatial distribution of the thickness of the first layer based on the borehole logging data

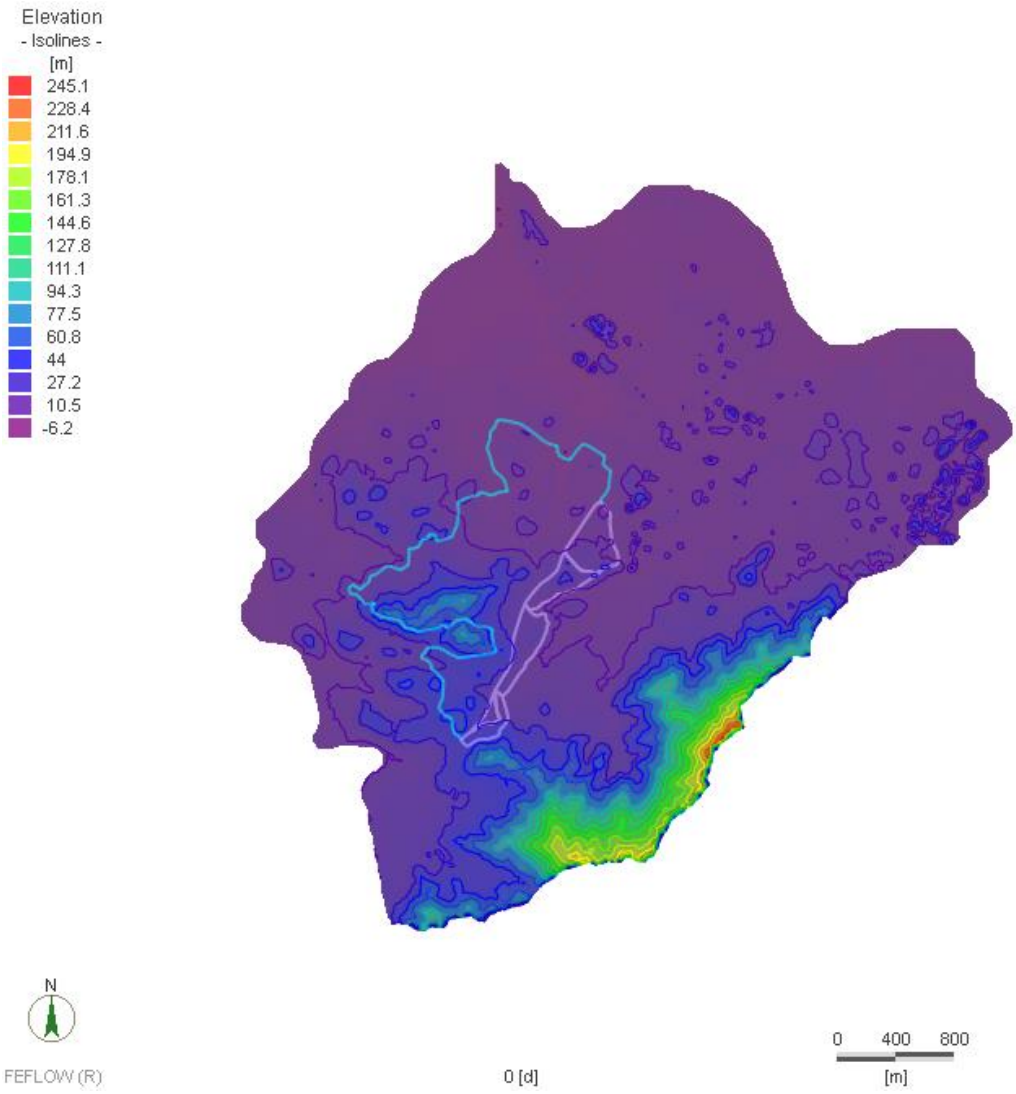

Figure 11. Bottom elevation of first layer in the 3D hydrogeological model.

Figure 12 illustrates the relation between the elevation of rock head (i.e. the bottom elevation of second layer) and the ground elevation. When the ground elevation is higher than 20 mPD, there is a linear relationship between the elevation of rock head and the ground elevation. This linear relationship is used to determine the elevation of rock head in the study area with no borehole data. However, when the ground elevation drops below 20 mPD, the relation between the elevation of rock head and the ground elevation is not clear, so the mean elevation of rock head of -15.5 mPD is used in the area with ground elevation lower than 20 mPD. Meanwhile, the elevations of rock head at the newly drilled borehole in sub-areas 1-4 are consistent with the linear relation as shown in Figure 12. Figure 13 shows the elevation data collected from CEDD library. Then the elevation of rock head in the 3D hydrogeological model is determined and shown in Figure 14

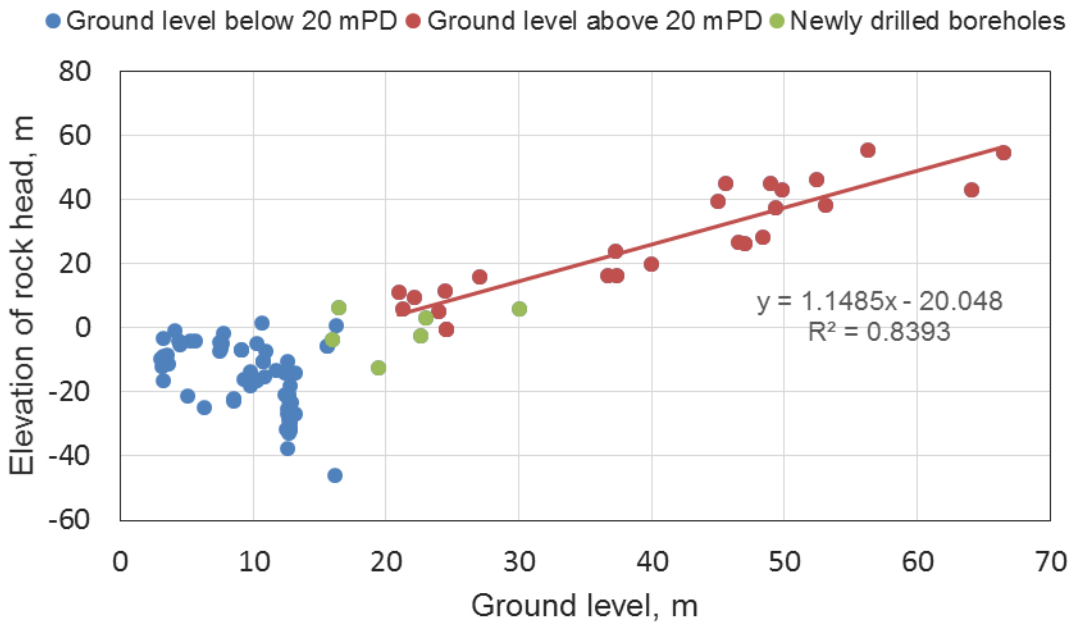

Figure 12. Relation between the elevation of bedrock and ground level from the borehole logging data.

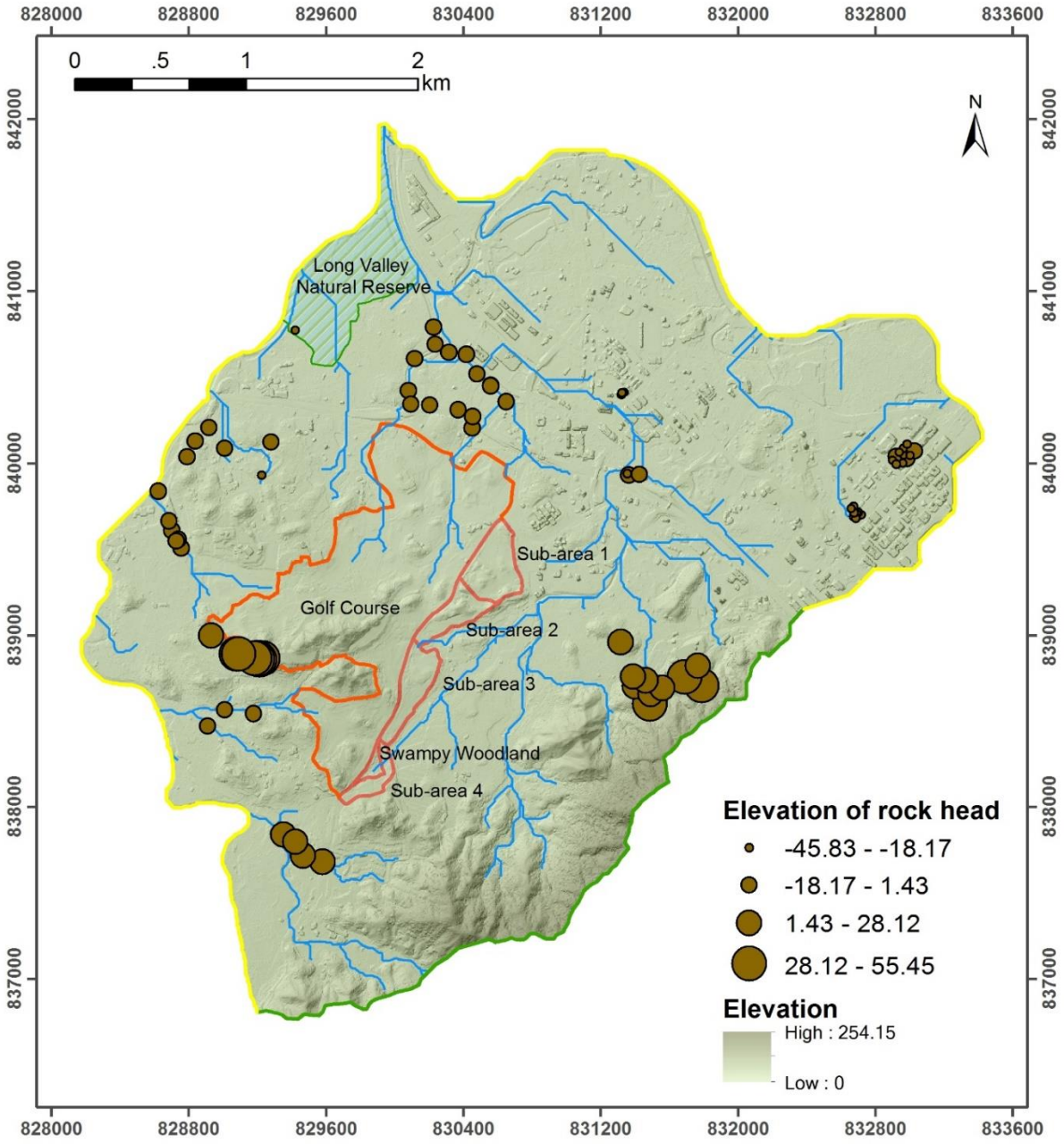

Figure 13. Spatial distribution of the elevation of rock head from the borehole logging data.

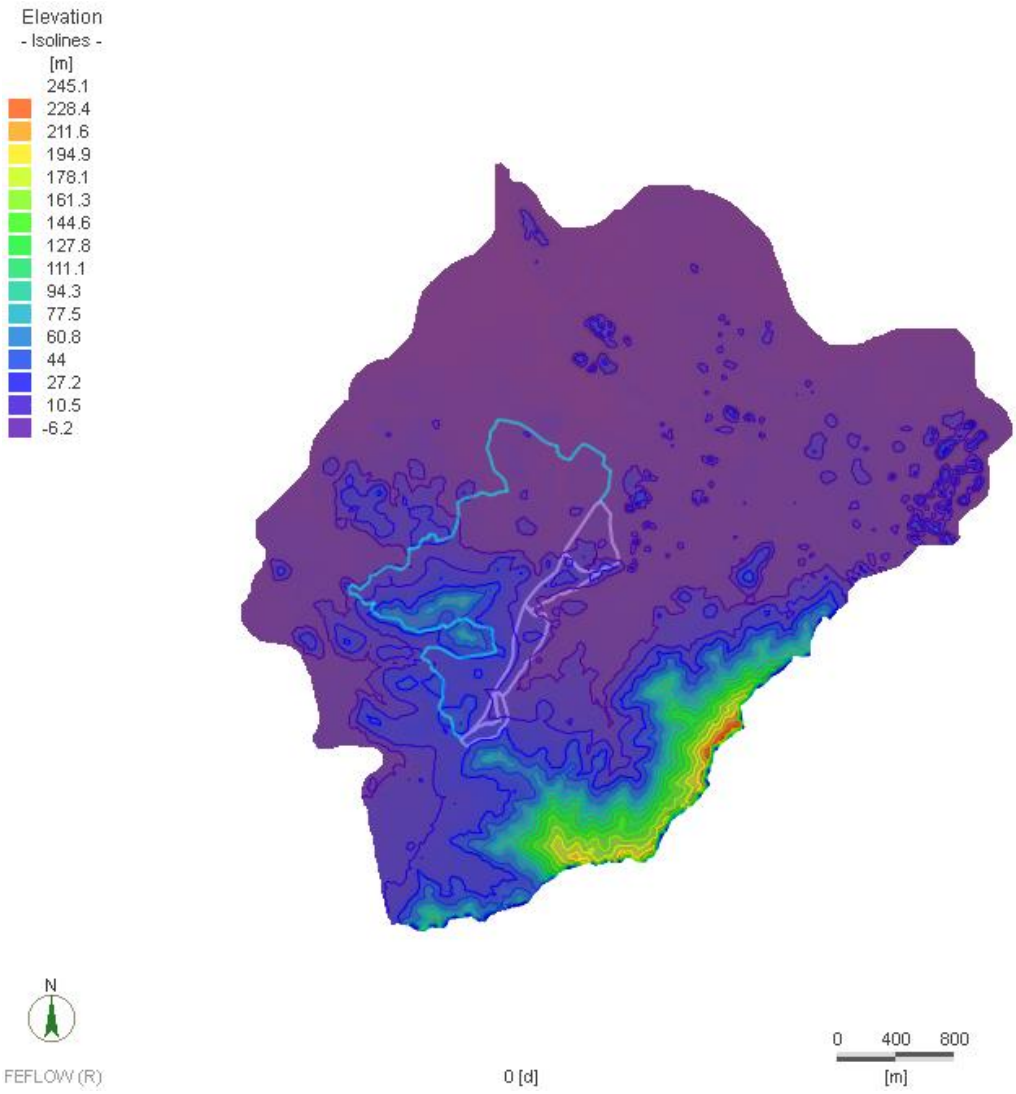

Figure 14. Elevation of rock head in the 3D hydrogeological model.

Finally, Figure 15 presents the constructed 3D hydrogeological model which will be employed to simulate groundwater flow in the study area. In the model, layer 3 is further divided into two layer for a better simulation of groundwater flow in the regions. The elevation of base of layer 3 is -50 mPD, and the elevation of base of layer 4 is -100 mPD.

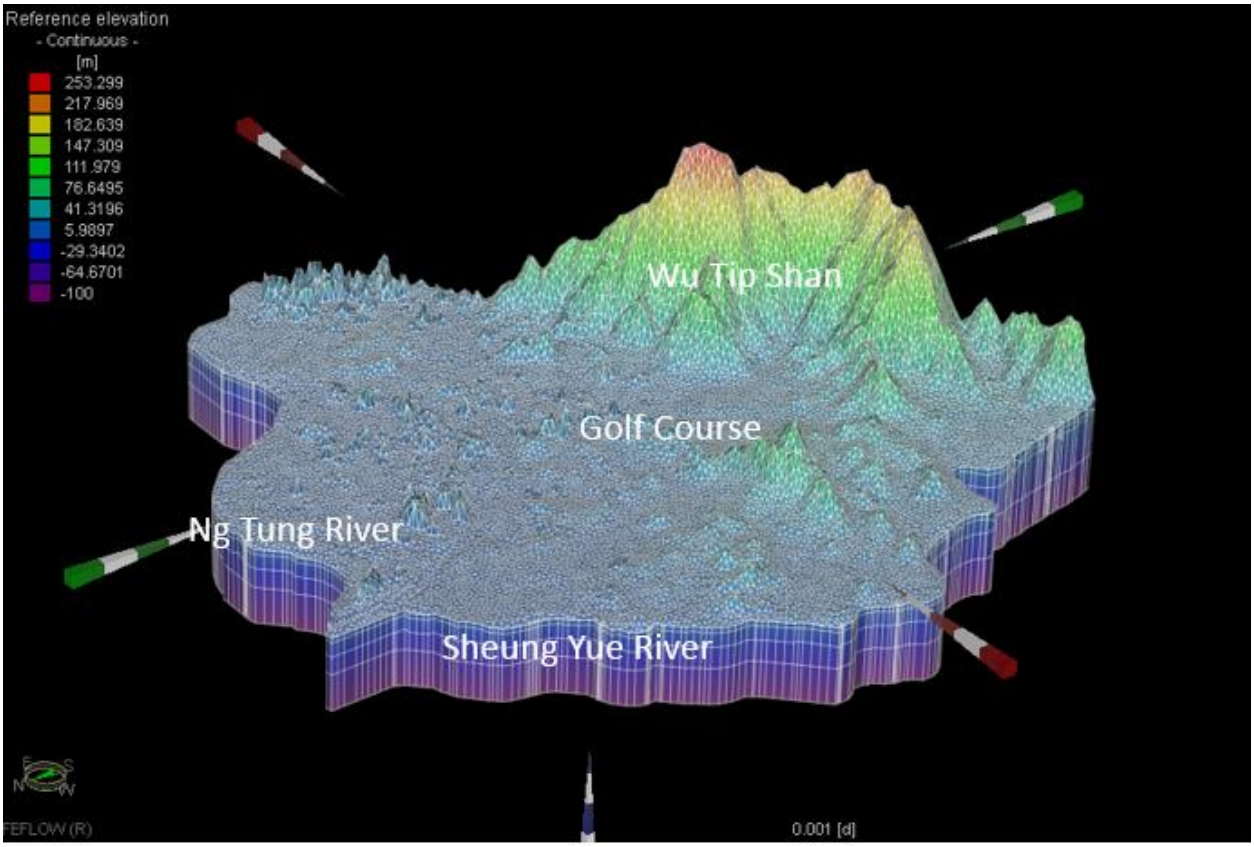

Figure 15. 3D hydrogeological model in the study area

3.2 Groundwater flow model

3.2.1 Governing equation of saturated groundwater flow

According to the mass conservation of fluid and Darcy's Law, the governing equation for saturated groundwater flow used in this study is:

$$S_s \frac{\partial h}{\partial t} = -\nabla \cdot (\boldsymbol{K} \nabla h + e) + Q_s$$

where S_s [L^{-1}] is the specific storage due to medium compressibility; $\boldsymbol{K}$ is the tensor of hydraulic conductivity for saturated medium; e is the gravitational unit vector; Q_s [L^3T^{-1}] is the flow of sources/sinks. The first term on the right-hand side of the equation is the Darcy flux of groundwater flow due to the hydraulic conductivity tensor and the gradient of the hydraulic head, and gravity.

Feflow, which is professional software for modeling groundwater flow, heat and mass transport processes in porous and fractured media, is employed to solve the governing equation.

3.2.2 Boundary conditions for the groundwater flow model

Boundary conditions are an essential component of any groundwater flow model. They describe the hydraulic behavior of the system at the boundary and control the flow of water into or out of the model domain. The boundary conditions can either be prescribed as head or flux values. In the case of the former, the head at the boundary is fixed, while for the latter, the flux (or flow rate) across the boundary is specified. In this study, there are two types of boundary conditions: no-flow boundary and given head boundary. The former refers to a situation where there is no flow across the boundary. Specifically, the Wu Tip Shan (Figure 15), which is the water divide of the catchment, is a no-flow boundary, while the Sheung Yue River and Ng Tung River (Figure 15) are given head boundaries.

3.2.3 Material properties

Material properties, including hydraulic conductivity, porosity, specific storage, and rainfall infiltration rate, are essential inputs for a groundwater flow model as they determine how easily water can flow through the subsurface materials. Inaccurate or imprecise material properties can lead to incorrect model predictions, making calibration of these properties critical for reliable groundwater modeling. In this study, the hydraulic conductivity and rainfall infiltration rate are the two parameters which have large uncertainties before calibrating the groundwater flow model; and the porosity and specific storage which have small uncertainties are prescribed before running the model.

According to the hydraulic conductivity data obtained from CEDD library, the K-sat data and the falling-head test data (Figures 3 and 4), the calibrated hydraulic conductivity values for the first and second layers of the model will be at the order of 10^{-5} m/s and 10^{-6}m/s respectively. However, the third and fourth layers have fixed values of 5×10^{-8} and 2×10^{-8} m/s, as the hydraulic conductivity of bedrock is quite small and has relatively less impact on the flow in the shallow zones.

As for the calibration of rainfall infiltration rate, it should be noted that, in a saturated groundwater flow model, both the hydraulic conductivity and rainfall infiltration rate have significant impacts

on the groundwater level. A high water level can be caused by either a large infiltration rate of rainfall or a small hydraulic conductivity. While several hydraulic conductivity data have been collected, the data on rainfall infiltration rate is not available. Consequently, the calibration of hydraulic conductivity will be restricted to a smaller range, as discussed earlier. The calibration of rainfall infiltration rate, on the other hand, is given a larger range during the calibration process.

3.3 Model calibration

As stated in section 3.2.3, the hydraulic conductivities for the first and second layers, as well as the rainfall infiltration rate, are the parameters to be calibrated. The calibration process aims to identify the best set of values for these parameters that can reproduce the observed water level data, as depicted in Figure 2. This will be achieved through a trial-and-error method, and the simulated water levels at different observation points will be compared with the corresponding measured data.

In this study, the calibration of the groundwater flow model will be performed in two scenarios: (1) model with uniform rainfall recharge rate, (2) model with non-uniform rainfall recharge rate. The results of the calibrated model will be further employed to predict the future water level change after partial development of Fanling golf course site in sub-areas 1-3.

3.3.1 Model with uniform rainfall recharge rate

In this scenario, the rainfall infiltration rate is set to be uniform at the surface of the first layer. The calibration results are presented in Figure 16, where the dots spread along the 1:1 line, indicating a reasonably good match between the simulated and monitored water levels. The Root-mean-square error (RMSE) is 3.57. The calculation of the flow budget of the model Shows that the net inflow/outflow is +0.0010 m^3/day, which is close to zero, indicating a small numerical error and a balanced water mass in the model.

The calibrated hydraulic conductivities for the first and second layers are $4x10^{-5}$ m/s and $4x10^{-6}$ m/s, respectively. The calibrated rainfall infiltration rate is 1% ($6x10^{-5}$ m/d) for a total rainfall rate of 2.2m/year.

The spatial distribution of hydraulic head and groundwater flow field in horizontal and vertical cross-section views are presented in Figures 17 and 19, respectively. The general flow direction in sub-area 1-4 is from sub-area 4 to sub-area 1 (i.e., from A to B).

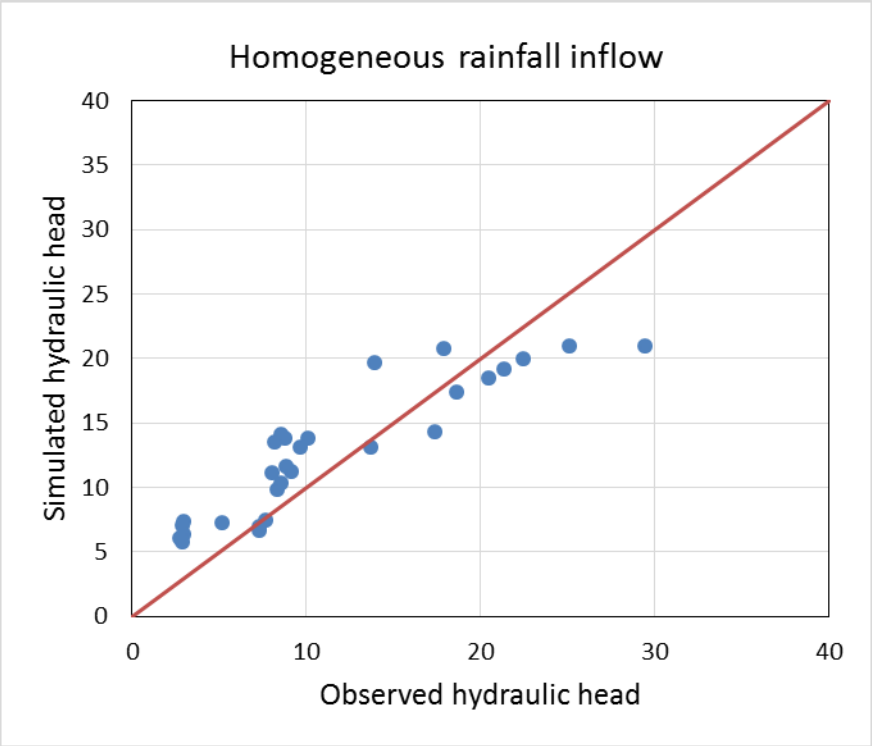

Figure 16. The calibration results of the model with uniform rainfall recharge rate

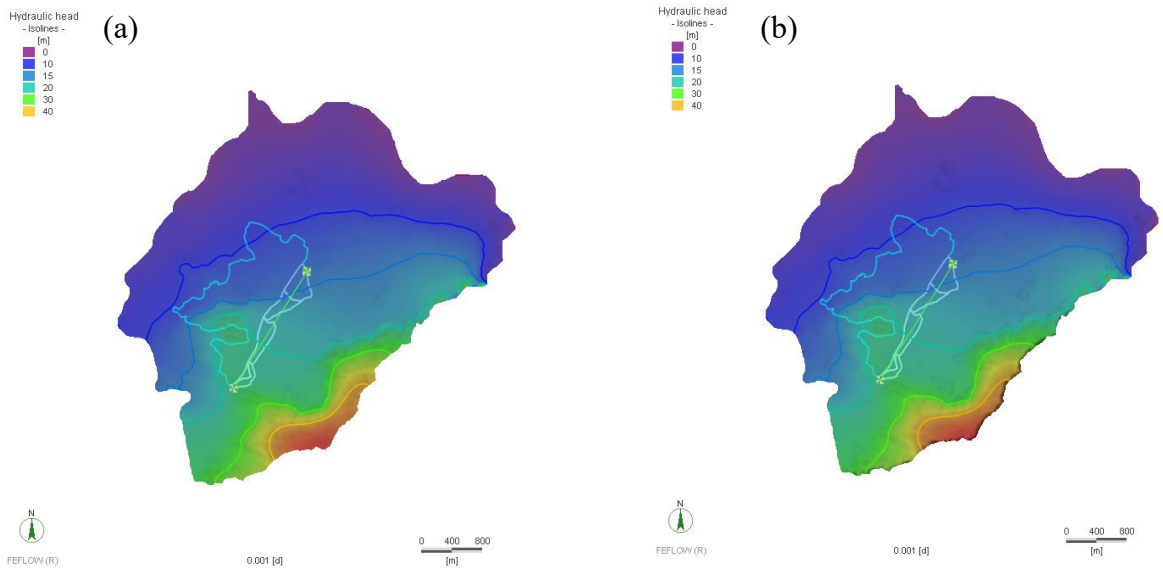

Figure 17 Horizontal cross section views of simulated hydraulic head of uniform rainfall recharge model: (a) layer 1, (b) layer 2.

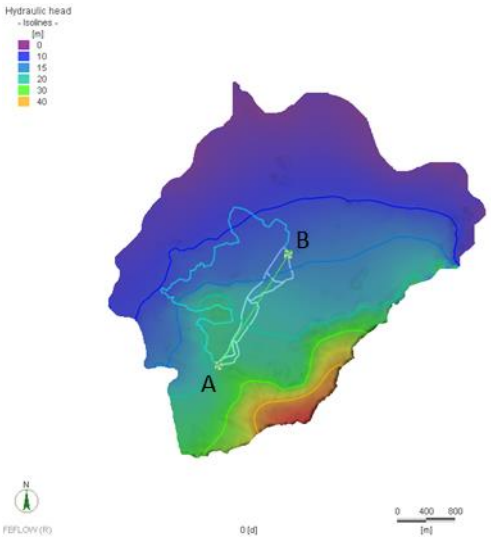

Figure 18 Location of cross section A-B for the vertical section view

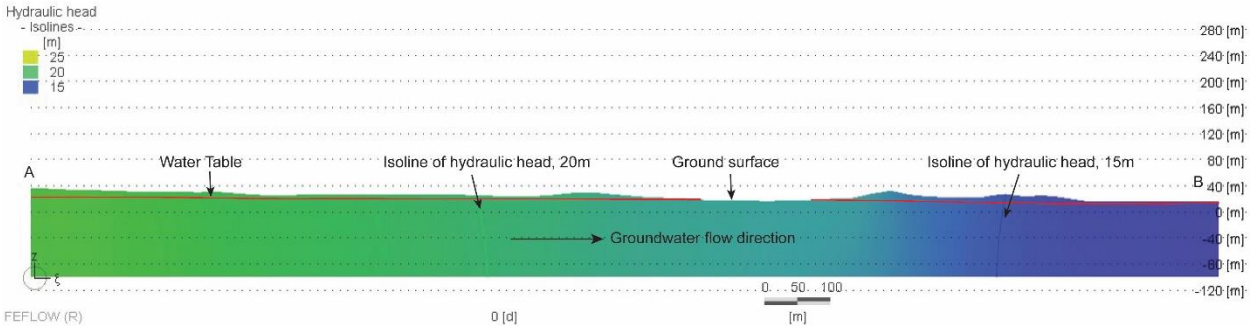

Figure 19 Vertical cross section view A-B of simulated hydraulic head of uniform rainfall recharge model.

3.3.2 Model with non-uniform rainfall recharge rate

The second scenario for the calibration of groundwater flow is the non-uniform rainfall recharge rate model. In this model, the rainfall infiltration rate varies spatially, with higher infiltration rate at higher elevations (elevation > 50 mPD) and lower infiltration at lower elevations (elevation < 50 mPD) due to the shallow water table depth at low elevation and the presence of discharge zones. Figure 20 shows the spatial variation of the rainfall infiltration rate.

The calibration results are shown in Figure 21, with a Root-mean-square error (RMSE) of 3.44, which is similar to the uniform rainfall recharge model. The calibrated parameters are the hydraulic conductivities of the first and second layers, which are 5x10-5 m/s and 5x10-6 m/s, respectively, and the rainfall infiltration rate at elevation>50 is 5% (3x10-4 m/d), while there is no infiltration at elevation<50. The flow budget of the model indicates a small numerical error, with the net inflow/outflow being -0.0004 m3/day. Figures 22 and 23 present the groundwater flow field in horizontal and vertical cross-section views, respectively. As the non-uniform rainfall recharge model is closer to the field situation, it will be used to predict the future water level changes after the partial development of Fanling golf course site in sub-areas 1-3.

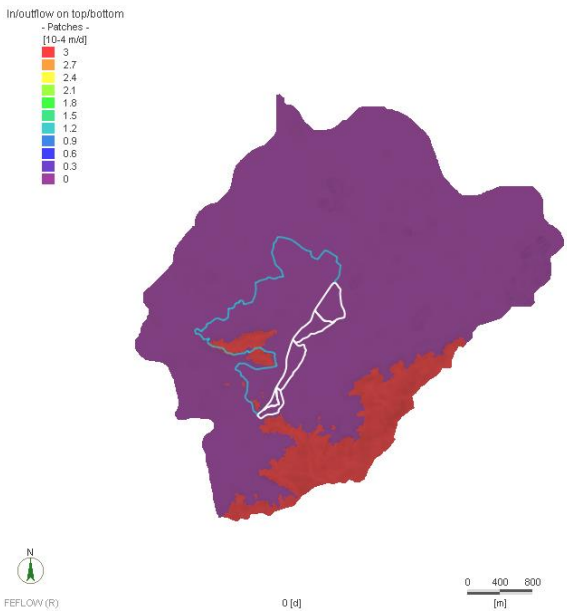

Figure 20. Spatial distribution of rainfall infiltration rate

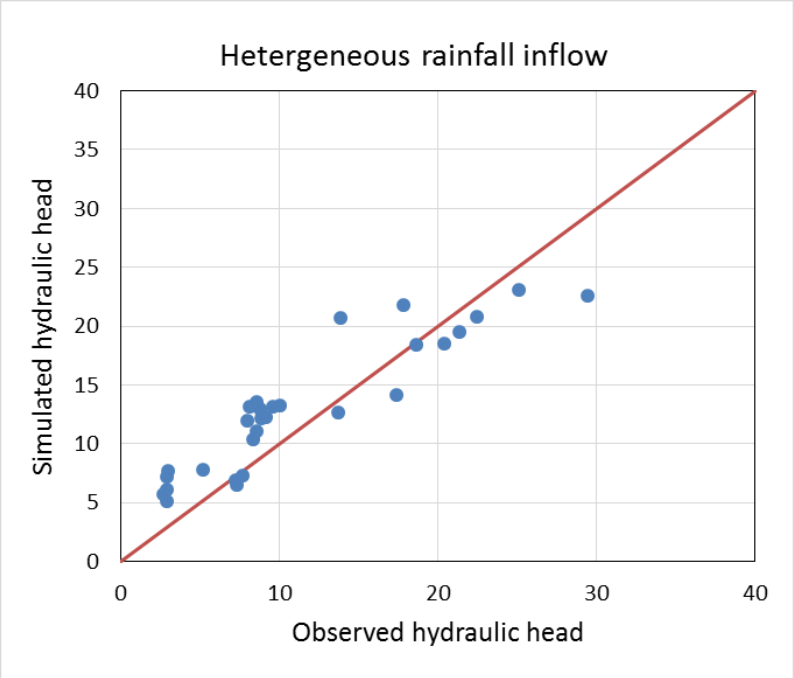

Figure 21. The calibration results of the model with non-uniform rainfall recharge rate

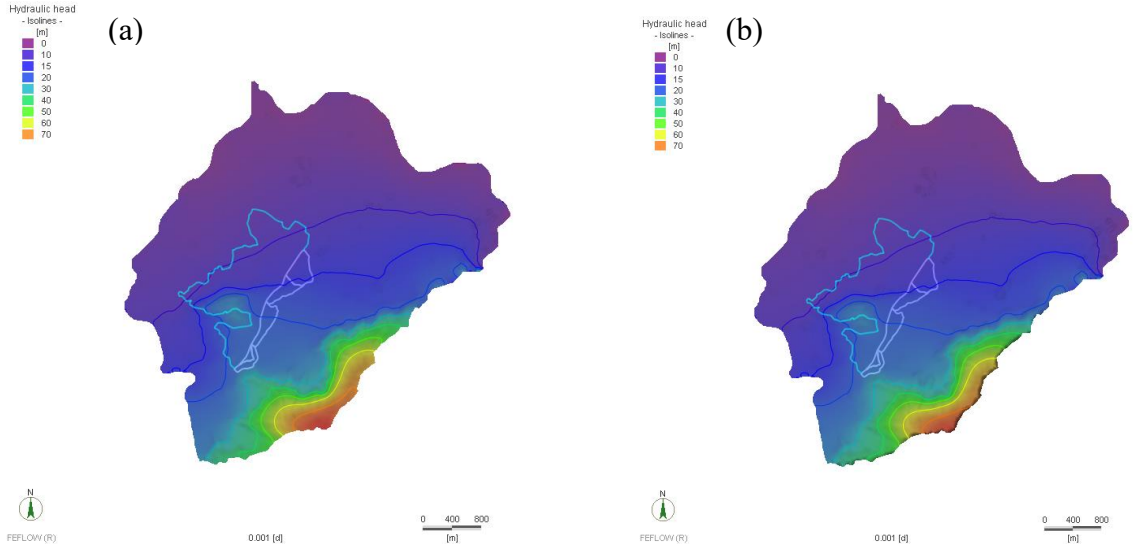

Figure 22. Horizontal cross section views of simulated hydraulic head of non-uniform rainfall recharge model: (a) layer 1, (b) layer 2.

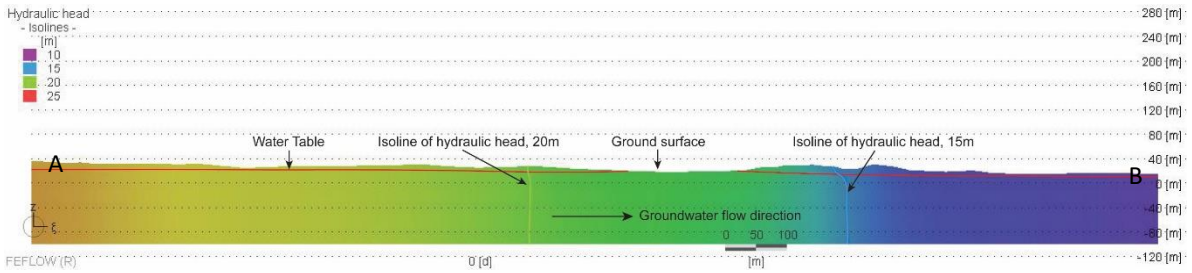

Figure 23. Vertical cross section view A-B of simulated hydraulic head of non-uniform rainfall recharge model.

3.3.3 Implication of the low rainfall infiltration rate in the study area

According to calibration results of two scenarios, the rainfall infiltration rates are quite low in both the uniform and non-uniform rainfall recharge models. This is due to the large low land area in the north of the model, where the water level is near the ground surface, making it difficult for rainwater to infiltrate to the water table. Instead, most rainwater becomes runoff.

This low infiltration rate has implications for potential flooding and sewage problems in the area. The flooding problem has been confirmed by previous reports, which state that "Ping Kong and the surrounding areas are prone to flooding in the wet season because of its low-lying topography (15-18 mPD) and deficiencies in the drainage system."

Meanwhile, the existence of natural ponds and lots of drainage channels at the golf course site also indicates the shallow water table and low rainfall infiltration rate in the study area.

3.4 Model predictions

After establishing the calibrated groundwater model, the future water level changes in the study area are investigated. Specifically, the influence of building foundation on the water level, as well as the combined effect of building foundation and tree planting are explored in this section. The analysis will provide insight into the potential impact of future development on the groundwater system, and help to identify strategies for the protection of Chinese swamp cypress in sub-area 4.

3.4.1 Influence of building foundation on water level change

In this section, the influence of building foundation on the water level change are investigated based on the calibrated groundwater flow model with non-uniform rainfall recharge. As shown in Figure 24, in sub-area 1, the hydraulic conductivity is set to be 5x10-8 m/s in both layers 1 and 2, representing the almost impermeable building foundation. The model result is presented in Figure 25.

By comparing the spatial distribution of hydraulic head in Figure 25, it can be found that the impact on the water level in the areas around sub-area 1, including sub-area 4 and Long Valley, is limited. The water flow around the impermeable area, and the water level at the upstream near sub-area 1 increases slightly. Although the influence of one building foundation is limited, it should be noted that if many building foundations are built downstream of sub-area 4, the water level will increase significantly as studied by [*Ding et al.*, 2008; *Jiao et al.*, 2006]. The detailed water level change will be discussed in section 3.4.3.

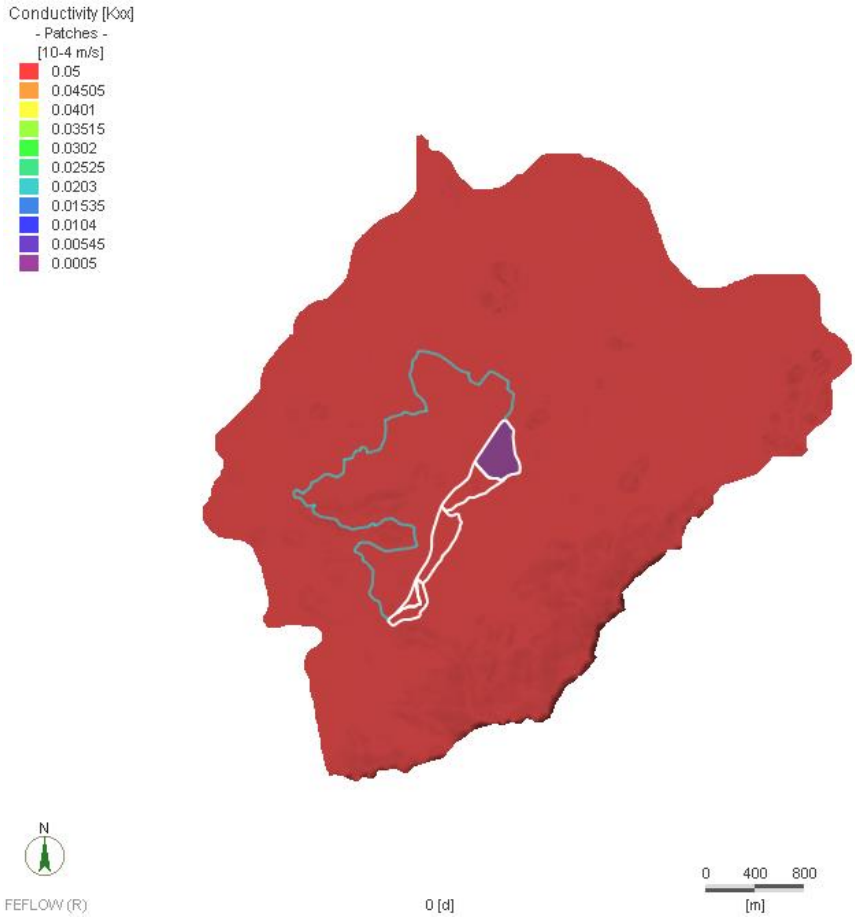

Figure 24 The hydraulic conductivity in the sub-area 1 after the construction of building foundation

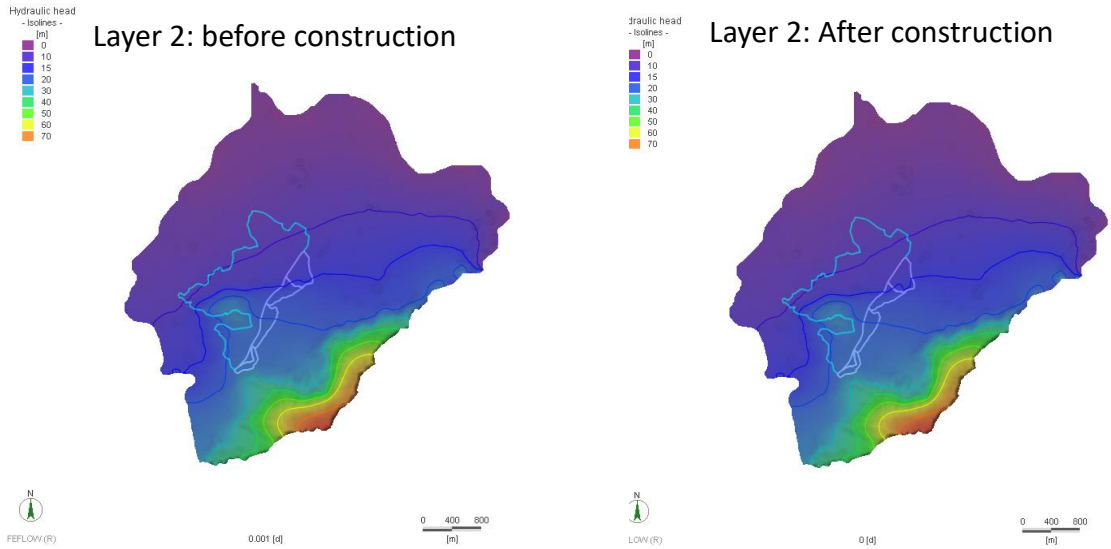

Figure 25 Comparison of hydraulic head before and after the construction of building foundation

3.4.2 Influence of building foundation and compensatory tree planting on water level change

The influence of building foundation and compensatory tree planting on water level change is investigated in this section using the calibrated groundwater flow model which is modified from the model in section 3.4.1 by adding an additional evapotranspiration (ET) rate in sub-areas 2 and 3.

In this study, the key problem is to determine the value of ET rate in sub-areas 2 and 3. According to the study of *Scott et al.* [2004], it can be referred that the ET increases from about 800mm/year to 1200 mm/year in Hong Kong with 2200 mm annual rainfall when the vegetation changes from grass to forest. Thus, the net increase of ET will be 400 mm/year. However, the tree planting does not cover all the sub-areas 2 and 3. Referring to the partial development plan in sub-areas 1-4, three~~wo~~ scenarios of compensatory tree planting are simulated in this study: (1) the compensatory tree planting area in sub-areas 2 and 3 is 1.5 times of the tree loss area which is 4.1 hectares in sub-area 1; (2) the compensatory tree planting area in sub-areas 2 and 3 equals the tree loss area, i.e., 4.1 hectares in sub-area 1; (3) the compensatory tree planting area in sub-areas 2 and 3 is 5.1 hectares.~~.~~

In the first scenario, the compensatory tree planting area will be 1.5 times of 4.1 hectares, i.e., 6.15 hectares. It should be noted that the total area of sub-areas 2 and 3 is 14.84 hectares. Then the mean

ET increases in sub-areas 2 and 3 is: 400x(6.15/(6.72+8.12))=165.76 mm/year. Similary, the mean ET in scenario 2 increases in sub-areas 2 and 3 is 400x(4.1/(6.72+8.12))=110.51 mm/year. In the third scenario, the ET increase in sub-areas 2 and 3 is 400x(5.1/(6.72+8.12))=137.45 mm/year.

Figure 26 shows the change of hydraulic head before and after building foundation and compensatory tree planting in the second scenario. It is found that the water level in sub-areas 2-4 decreased apparently significantly, but the general flow direction in the modeling area does not change much. The detailed water level change will be discussed in section 3.4.3.

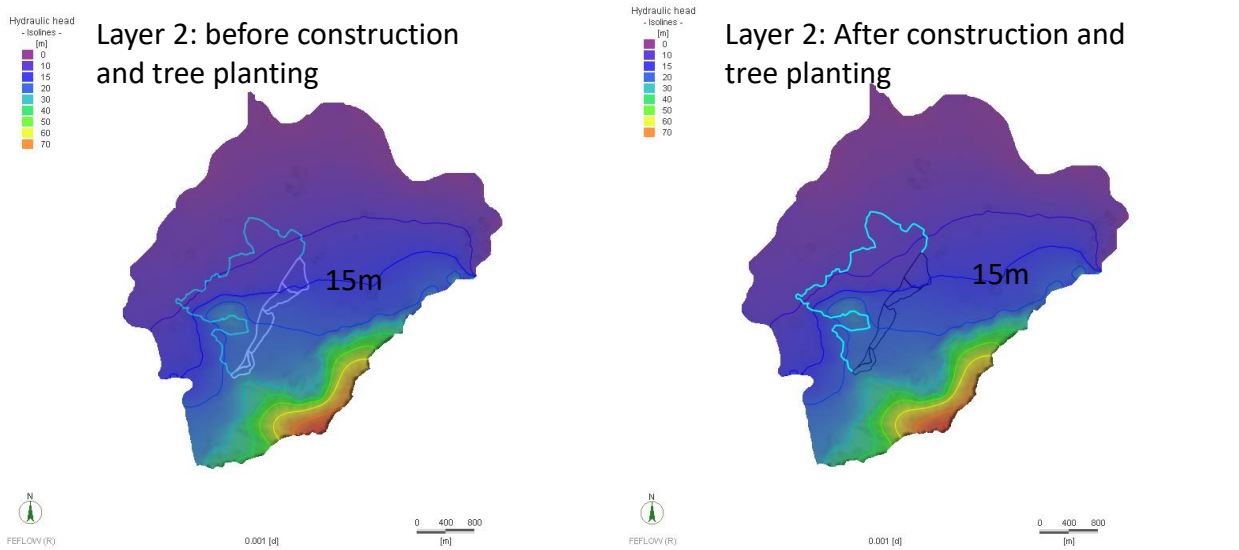

Figure 26 Comparison of hydraulic head before and after the construction of building foundation and compensatory tree planting

3.4.3 Water level change before and after partial development of Fanling golf course site

In this section, the influence of building foundation and compensatory tree planting on water level change is further elaborated. To illustrate the impact clearly, five observation points were set up in the groundwater flow model, located at Long Valley and sub-areas 2-3 (Figure 27).

Table 2 lists the simulated water level in different models at the four observation points. From the table, it can be seen that after the construction of building foundation, the water level increases slightly at points B, C, and D. However, after compensatory tree planting, the water level decreases significantly at points B, C, and D, which are located at the upstream of sub-area 1. The water level decreases in these three points can be as much as about 0.7 m. At point A and E, which are located at the downstream of sub-area 1, the water levels decrease slightly after the construction

of building foundation, and the water levels decrease further more after tree planting. These results suggest that compensatory tree planting has significant water level decrease at sub-areas 2-3.

With reference to the study of *Zhang and Fischer* [2021], the Chinese Swamp Cypress grows in flat, seasonally or permanently flooded areas of river systems, lakes or ponds from sea-level up to 900 m. In these areas, the water table plays a crucial role in the growth and survival of this species, and the trees can tolerate both seasonally and permanently flooded conditions. However, they may not survive in areas with a low water table. According to the simulated results in Table 2, the tree planting has the largest influence on the decrease of water table, threating to the survival of the species.

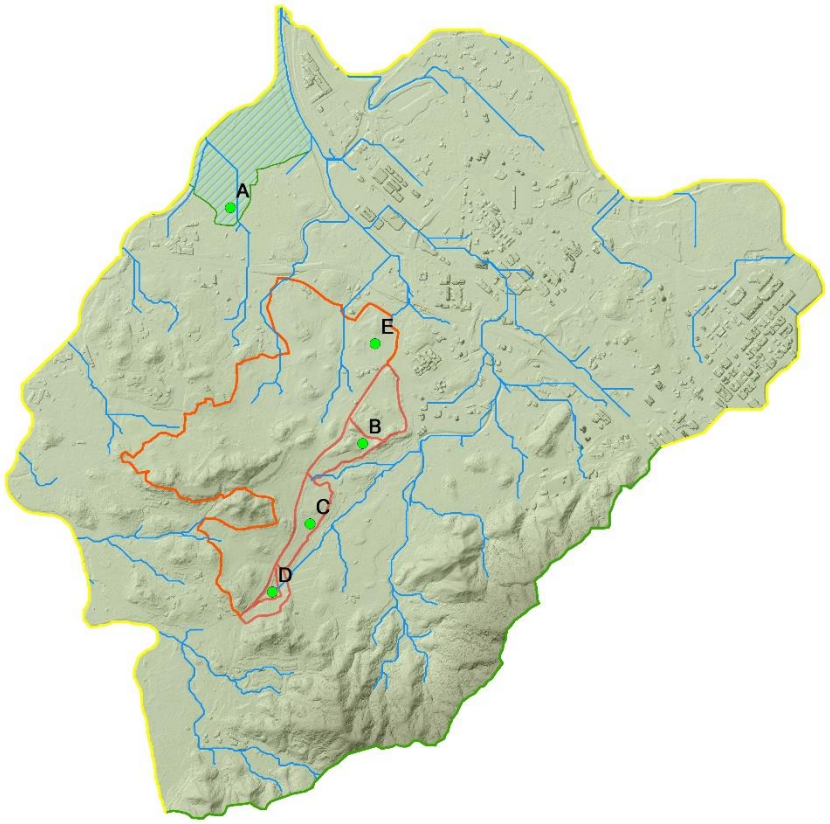

Figure 27. Observation points set in the numerical model

Table 2. Water level changes at the observation points

Observation point	A	B	C	D	E

Before construction	3.85 m	16.66 m	20.76 m	22.05 m	10.70 m
After construction	3.81 m	16.84 m	20.86 m	22.12 m	10.56 m
After construction and tree planting(4.1 ha)	3.66 m	15.74 m	19.93 m	21.38 m	10.06 m
After construction and tree planting(6.15 ha)	3.59 m	15.10 m	19.42 m	21.00 m	9.80 m
After construction and tree planting(5.1 ha)	3.63 m	15.43 m	19.70 m	21.21 m	9.94 m

4 CONCLUSIONS

This study assesses the ecological impact of proposed public housing and infrastructure development at Fanling Golf Course on the groundwater flow system in the surrounding areas by developing a 3D regional groundwater flow model. Among the areas, the ecological value of sub-areas 2-4 and the Long Velley Nature Reserve are evaluated to be moderate to high. Notably, sub-area 4 is home to 38 endangered Chinese swamp cypresses that require a specialized habitat and are sensitive to changes in the water table.To establish the groundwater flow model, three types of data are collected, which include borehole logging, water level, and hydraulic conductivity data from CEDD library, K-sat experiment and falling-head test at FGC. The hydraulic conductivity and rainfall infiltration rate are the two parameters to be calibrated by the models with uniform rainfall recharge and non-uniform rainfall recharge. The calibrated hydraulic conductivity values for the first and second layers of the model are at the order of 10^{-5} m/s and 10^{-6} m/s, respectively. The calibrated rainfall infiltration is 1% in the model with uniform rainfall recharge, and 5% at the elevation above 50 mPD in the model with non-uniform rainfall recharge. The low rainfall infiltration rate is consistent with high risk of flooding problem in the model area.

The groundwater flow model is used to simulate the water level changes in East FGC before and after the construction of buildings in sub-area 1 and the compensatory tree planting in sub-areas 2-3. The model predictions indicate that the construction of buildings in sub-area 1 would result in a slightly increase in water levels in the upstream of sub-area 1. However, compensatory tree

planting in sub-areas 2 and 3 can lead to about 0.7 m decrease of water level in sub-areas 2-4, which may influence the hydrological environment for the living of Chinese swamp cypress .

5 COMMENTS ON CHAPTER 7 OF THE EIA REPORT

We read Chapter 7 of the EIA report and have the following comments.

This chapter includes five conclusions. The first two conclusions essentially state that the proposed housing development in Sub-Area 1 and the compensatory tree planting in Sub-Area 3 would not impact the sources of surface water and groundwater for the swampy woodland in Sub-Area 4. These statements are correct; however, they can be inferred solely by examining the topographic map. As Sub-Area 1 is downstream of Sub-Area 4, it is evident that any development in Sub-Area 1 will not affect the sources of surface water and groundwater in Sub-Area 4.

Although the "sources" of surface water and groundwater in Sub-Area 4 will not be affected by the housing development in Sub-Area 1 and the compensatory tree planting, this does not mean that these activities will not impact the water regimes in Sub-Area 1. They will modify the water regimes by changing the conditions of groundwater discharge. The housing development, with deep foundations consisting of almost impermeable construction materials down to the bedrock, will hamper groundwater discharge, potentially elevating the water table upstream. The compensatory tree planting will have the opposite effect, that is, to increase groundwater discharge, potentially leading to a decrease in the water table in Sub-Area 1. Unfortunately, these issues are not touched upon in the report.

The last three conclusions essentially state that if there is any water loss due to housing development or tree planting, water can be added to the affected areas since there is sufficient reclaimed water available. These conclusions can be made without conducting any research.

However, putting this plan into action is no easy feat, as the saying goes, "the devil is in the details". The Chinese Swamp Cypress have adapted well to the current water environment, specifically the

water table depth and its variation. Even assuming that all the estimate figures (406 m3/day, 37 m3/day, etc) are correct, the challenge remains of determining when, where, and how much water to add to ensure the preservation or restoration of the original water environment, particularly the water table in the area with the Swamp Cypress. Another aspect of concern is guaranteeing sufficient irrigation for the planted area, given the varying rates of evapotranspiration and water demand of the trees over time.

The depth of infiltrated rainwater for different types of soils was modeled using the Green-Ampt infiltration method (Section 7.5.4). This method is simplified vertical one dimensional infiltration model focusing on the infiltration in the shallow unsaturated zone (https://open.library.okstate.edu/rainorshine/chapter/6-2-green-ampt-infiltration-model/). The Storm Water Management Model (SWMM) is a dynamic rainfall–runoff–subsurface runoff simulation model (https://en.wikipedia.org/wiki/Storm_Water_Management_Model) and is not about groundwater flow in saturated zones. This model cannot provide any information on the water table change due to housing development and water loss from tree planting. The root system of Swamp Cypress is below water table, so the water table information is more important than soil moisture above the water table.

Hydrogeology and groundwater regime in these areas, especially in the Sub-Area 1 are very important. Because SWMM is not about groundwater flow and hydrogeology. Their discussion is not based on the geology and hydrogeology of the site.

It seems that the infiltration rate is too high, averaging about 1.5 m/yr. With a porosity of about 0.3, this implies that the water table must rise by 5 m, or there must be an unsaturated zone of 5 m to accommodate the infiltrated water. However, many areas have a high water table almost near the land surface, making it difficult to find enough soil space to handle such a significant volume of water per year.

Furthermore, the infiltration test was conducted in November, which is the dry season. Therefore, it is possible that the infiltration rate may have been overestimated. During the wet season, when the soil is wetter and the water table is higher, the infiltration rate may be lower. We need to know the net rainfall recharge after considering evatransporation, but it is unclear how the net infiltratgion could be if evatransporation is considered from their report.

REFERENCES

Civil Engineering and Development Department (CEDD) (2019), Technical Study on Partial Development of Fanling Golf Course Site - Feasibility Study*Rep.*

Ding, G., J. J. Jiao, and D. Zhang (2008), Modelling study on the impact of deep building foundations on the groundwater system, Hydrological Processes: An International Journal, 22(12), 1857-1865.

Equipment, E. A. (2004), Compact constant head permeameter: user's manual, Giesbeek: Eijkelkamp Agricultural Equipment.

Jiao, J. J., X.-S. Wang, and S. Nandy (2006), Preliminary assessment of the impacts of deep foundations and land reclamation on groundwater flow in a coastal area in Hong Kong, China, Hydrogeology Journal, 14(1), 100-114.

Scott, D., L. Bruijnzeel, R. Vertessy, and I. Calder (2004), Impacts of Forest plantations on streamflow, Encyclopedia of Forest Science, 367-377.

Zhang, J., and G. A. Fischer (2021), Reconsideration of the native range of the Chinese Swamp Cypress (Glyptostrobus pensilis) based on new insights from historic, remnant and planted populations, Global Ecology and Conservation, 32, e01927.